Modeling realistic scattering from Born-von Karman phonons in copper and pyrolytic graphite with McStas

Kristine M. L. Krighaar[a], Kim Lefmann[a]

[a]*Nanoscience Center, Niels Bohr Institute, University of Copenhagen, Universitetsparken 5, DK-2100 Copenhagen Ø, Denmark*

Abstract

We present the implementation of Born-von Karman phonon scattering in the neutron ray-tracing simulation package McStas. We present the Born-von Karman calculations and the implementation of Monte Carlo sampling of scattering from a dispersion surface. We demonstrate the use of this new McStas component by virtual experiments, and show that they compare well to literature results on copper and pyrolytic graphite.

1. Introduction

The neutron ray-tracing scattering package McStas was inaugurated in 1997 [1] and has now developed to become a generally accepted tool for modeling neutron scattering instrumentation, from the transport properties of guides, over design of optical elements to resolution functions of full instruments and complete virtual experiments [2, 3, 4]. Many different scattering processes have been modeled in McStas to enable the description of both scattering from different types of sample and background scattering properties of materials. Simulation of the latter has been strongly enabled by the release of the `Union` component in McStas that is able to combine different types of scattering into the same material component [5, 6].

Inelastic scattering from crystals has so far only been sporadically implemented in McStas. The present version of McStas contains only a very rudimentary phonon component, `Phonon_simple`, that contains a single longitudinal acoustic mode on the fcc lattice. For non-crystalline samples (powders or liquds), however, components exist that model inelastic scattering. We here mention two: A) an incoherent quasielastic scatterer, `Tunneling_sample`, introduces a Lorentzian broadening of the incoherent elastical line. B) the general inelastic powder/liquid component `Isotropic_Sqw` uses a tabularized scattering function $S(q, \omega)$, given as user input [7].

In this work, we address the clear lack of single-crystal inelastic scattering samples in McStas by presenting a new component, `Phonon_BvK`, that models the scattering from phonons calculated from Born-von Karman force constant theory [8]. The model includes both longitudinal and transverse force constants

and allows for flexible neighbour settings, enabling different lattice geometries. The component calculates both the dispersion surface and the phonon polarization from the force constants. We show that the modeled phonon dispersions for metallic copper and pyrolitic graphite with force constants up to 4'th nearest neighbours compare very favourably with experimental results from literature. We present the results of McStas simulations on a virtual triple-axis instrument and demonstrate that both dispersions, intensities, and polarization factors are correctly reproduced by the new `Phonon_BvK` component.

? OR SHOULD IT BE TWO SEPARATE COMPONENTS ?

As an introduction to the new component and its function, we present briefly the Born-von Karman theory. We also present the implementation of Monte-Carlo sampling from a dispersion surface that is essential for the simulations performed. This sampling method has been used in McStas for two decades, in `Phonon_simple`, but was not published earlier.

2. Born-von Karman theory for phonons

More than a century ago, M. Born and T. von Karman presented their classical model of atomic lattice vibrations [8] that today stands as one of the solid foundations of phonon theory CITE TEXTBOOK. Within this model, it is assumed that forces in all three dimensions depend linearly on the displacement of atoms from their equilibrium (lattice) positions, $\mathbf{u}_i(t)$, relative to the positions of their neighbouring atoms, $\mathbf{u}_j(t)$. We write the force on atom i from atom j as

$$F^{\alpha}_{i,j}(t) = \Phi^{\alpha\beta}_{i,j} \times (-u^{\beta}_{i}(t) + u^{\beta}_{j}(t)), \tag{1}$$

where α and β are cartesian coordinates. $\Phi_{i,j}$ represent the three dimensional force constant matrix between atoms i and j, showing that the theory includes cross terms, *e.g.* that a displacement along the x-direction could give a force component also in the y-direction. For simplicity, we here use the axially symmetric approximation, where the force constant matrix is diagonal in a coordinate system that has one main axis along the line between the two atoms.

To study the classical vibration modes of the lattice, we invoke Newtons second law for atom i:

$$M_i \frac{d^2\mathbf{u}_i(t)}{dt^2} = \sum_j F^{\alpha}_{i,j}(t). \tag{2}$$

We use equation (1) to determine the forces and assume that the motion of the atoms consists of harmonic plane waves

$$\mathbf{u}_i(t) = \mathbf{u}_0 \exp(i\mathbf{q}' \cdot \mathbf{r}_i) \exp(-i\omega_{q',p}t), \tag{3}$$

with $\mathbf{q}$' being the propagation vector and $\omega_{q',p}$ the frequency, where in turn p is a labeling of the different modes at one value of $\mathbf{q}$'.

2.1. Phonons in a Bravais lattice

Initially, we consider vibrations a Bravais lattice, *i.e.* one atom per unit cell. With these assumptions, we follow Ref. [9] to reach the equations of motion for atom i:

$$M\omega_{q',p}^2 u_i^\alpha(t) = \sum_\beta D^{\alpha\beta}(\mathbf{q}) u_i^\beta(t), \tag{4}$$

where the Fourier transformed force constant matrices are given by

$$D^{\alpha\beta}(\mathbf{q}') = \sum_j \Phi_{i,j}^{\alpha\beta} \times (1 - \exp[i\mathbf{q}' \cdot (\mathbf{r}_j - \mathbf{r}_i)]). \tag{5}$$

Since a Bravais lattice has inversion symmetry, the sum can be transformed into pairs $\mathbf{r}_{i,j}$ and $-\mathbf{r}_{i,j}$, making the result purely real:

$$D^{\alpha\beta}(\mathbf{q}') = \sum_j \Phi_{i,j}^{\alpha\beta} \times (1 - \cos[\mathbf{q}' \cdot (\mathbf{r}_j - \mathbf{r}_i)]), \tag{6}$$

The solutions to the equations of motion are found for each value of $\mathbf{q}$' by finding the three polarization directions $\mathbf{e}_{q',p}$ that solve the eigenvalue equation

$$\omega_{q',p}^2 \mathbf{e}_{q',p} = \frac{1}{M} \mathcal{D}(\mathbf{q}') \mathbf{e}_{q',p}, \tag{7}$$

where the eigenvalues are the squares of the corresponding vibration frequencies, $\omega_{q',p}$.

2.2. Phonons in a non-Bravais lattice

In a lattice with an n-atom basis, each atom in the basis will have its own set of equations of motion, and the generalized version of (4) becomes

$$M_\Delta \omega_{q',p}^2 u_{\Delta,i}^\alpha(t) = \sum_{\beta,\Delta'} D_{\Delta,\Delta'}^{\alpha\beta}(\mathbf{q}) u_{\Delta,i}^\beta(t), \tag{8}$$

where Δ and Δ' labels the different atoms in the unit cell. The Fourier transformed force constant matrices are now given by

$$D_{\Delta,\Delta'}^{\alpha\beta}(\mathbf{q}') = \sum_j \Phi_{\Delta,\Delta',i,j}^{\alpha\beta} \times (1 - \exp[i\mathbf{q}' \cdot (\mathbf{r}_{\Delta',j} - \mathbf{r}_{\Delta,i})]). \tag{9}$$

The vector space that we here work in should be understood as $3n$-dimensional, with the displacement vector being $\mathbf{u} = (\mathbf{u}_1, \mathbf{u}_2, ..., \mathbf{u}_n)$. This makes the matrix $\mathcal{D}(\mathbf{q}')$ have the dimension $(3n \times 3n)$. Except this enlargement of the dimensionality, the polarization directions and vibration frequencies are still given by the solutions to the eigenvalue equation (7). REFERENCE TIL TEKSTBOG

HVORDAN SKRIVER VI HVIS MASSERNE ER FORSKELLIGE?

3. Implementation of Monte Carlo sampling from dispersion surfaces

3.1. Neutron scattering and probabilities

We start by defining the neutron scattering vector

$$\mathbf{q} = \mathbf{k}_\mathrm{i} - \mathbf{k}_\mathrm{f}, \tag{10}$$

where $\mathbf{k}_\mathrm{i}$ and $\mathbf{k}_\mathrm{f}$ represent the wave vectors for the incoming and outgoing neutron, respectively. In analogy, we define the neutron energy transfer by

$$\hbar\omega = E_\mathrm{i} - E_\mathrm{f} = \frac{\hbar^2}{2m}(k_\mathrm{i}^2 - k_\mathrm{f}^2), \tag{11}$$

where E_i and E_f are the energies of the incoming and outgoing neutrons, respectively. Inelastic scattering is described by the partial differential cross section, given by

$$\frac{d^2\sigma}{d\Omega dE_\mathrm{f}} = \frac{\text{neutrons per sec. in } d\Omega dE_\mathrm{f}}{\Psi d\Omega dE_\mathrm{f}}, \tag{12}$$

where Ψ is the incoming neutron flux, $d\Omega$ is the (small) solid angle of scattering considered and $dE_\mathbf{f}$ is a (small) interval for the outgoing neutron energy [10]. Integration over all values of E_f gives us the differential cross section, known mostly from neutron diffraction, but also highly relevant in this context:

$$\frac{d\sigma}{d\Omega} = \frac{\text{neutrons per sec. in } d\Omega}{\Psi d\Omega}. \tag{13}$$

Scattering cross sections from samples are in general proportional to the sample size. For this reason, we here define the volume-specific partial cross sections $d\Sigma/d\Omega = V^{-1}d\sigma/d\Omega$, where V is the sample volume, and similar for $d^2\Sigma/d\Omega dE_f$.

For a sufficiently thin sample, the beam is not noticeably attenuated, and we can assume Ψ constant through the sample. Without loss of generality, we assume the sample to be (locally) box shaped with A and L are the area and thickness of the sample perpendicular to the beam, and $V = AL$. We can now write the scattering probability for neutrons to go into a solid angle element $\Delta\Omega$ as the ratio of the scattered and the incoming neutron intensities:

$$P(\Delta\Omega) = \frac{\text{neutrons per sec. in } \Delta\Omega}{A\Psi} = \frac{d\Sigma}{d\Omega}\Delta\Omega L. \tag{14}$$

3.2. Sampling of scattering from dispersions

We assume that we have a single crystal sample, in which excitations are governed by a number of dispersion relations, $\hbar\omega_i = d_i(\boldsymbol{q}')$. This implies that the excitations are confined in a finite number of three-dimensional sheets within the four-dimensional $(\hbar\omega, \boldsymbol{q}')$ space. This is *e.g.* the case for phonons. For simplicity, we consider first a single dispersion branch, $d_1(\boldsymbol{q}')$ and later generalize the expressions to several branches, d_i.

From conservation of energy and momentum, neutrons can be scattered only when both $\mathbf{q}$ and $\pm\hbar\omega$ of the neutron matches that of the dispersion. The plus-minus sign represents the fact that a quasiparticle can both be created and annihilated. Thus the partial differential cross section for inelastic scattering can be written as

$$\frac{d^2\sigma}{d\Omega dE} = W_{\pm}(\boldsymbol{q}, \hbar\omega)\delta[\hbar\omega \pm d_1(\pm\boldsymbol{q}')] \tag{15}$$

where $W_{\pm}(\hbar\omega)$ is a weight function that depends on the physics of the problem.

To obtain a cross section expression without δ functions, we integrate Eq. (15) over the final energy, E_{f}, for a fixed neutron direction, $\hat{k}_{\mathrm{f}}$ to obtain the differential cross section

$$\begin{aligned}\frac{d\sigma}{d\Omega}(\hat{k}_{\mathrm{f}}) &= \int_{-\infty}^{\infty} W(\boldsymbol{q}, \hbar\omega)\delta\left(\frac{\hbar^2}{2m}(k_{\mathrm{i}}^2 - k_{\mathrm{f}}^2) - d_1(\mathbf{k}_{\mathrm{i}} - k_{\mathrm{f}}\hat{\mathbf{k}}_{\mathrm{f}})\right) d\left[\frac{\hbar^2 k_{\mathrm{f}}^2}{2m}\right] \\ &= \sum_{j=1}^{l} W(\boldsymbol{q}_j, \hbar\omega_j)\frac{\hbar^2 k_{\mathrm{f},j}}{mJ(k_{\mathrm{f},j})},\end{aligned} \tag{16}$$

where the index j runs over the l possible solutions to the kinematic constraint (11), using a single dispersion relation, d_1, and one particular choice of $\hat{\mathbf{k}}_{\mathrm{f}}$. As shown by Squires [10], there is always at least one solution to the kinematic constraint, on the energy gain side. In practice l lies in the range 1 to 3. In the calculations above, we have utilized $\int \delta(f(x))dx = \sum_j \left[(df/dx)(x_j)\right]^{-1}$, and have defined the Jacobian of the coordinate transformation

$$J(k_{\mathrm{f},j}) = \frac{\partial}{\partial k_{\mathrm{f}}}\left[\frac{\hbar^2}{2m}(k_{\mathrm{i}}^2 - k_{\mathrm{f}}^2) - d_1(\mathbf{k}_{\mathrm{i}} - k_{\mathrm{f}}\hat{\mathbf{k}}_{\mathrm{f}})\right] \tag{17}$$

From Eq. (17) we notice that if $d_1(\boldsymbol{q}) = 0$ (the elastic condition), then $mJ(\mathbf{k}_{\mathrm{f},j}) = \hbar^2 k_{\mathrm{f},j}$, and eq. (16) would reduce to $d\sigma/d\Omega(\mathbf{q}) = W_1(\boldsymbol{q}, \hbar\omega)$, as expected *e.g.* from diffraction.

3.3. The case of phonon scattering

The inelastic phonon cross section for a Bravais crystal is given by Ref. [10, ch.3]

$$\begin{aligned}\frac{d^2\sigma'}{d\Omega dE_{\mathrm{f}}} &= b^2\frac{k_{\mathrm{f}}}{k_{\mathrm{i}}}\frac{(2\pi)^3}{V_0}\frac{1}{2M}\exp(-2W) \\ &\times \sum_{\tau,q',p}\frac{(\mathbf{q}\cdot\mathbf{e}_{q',p})^2}{\omega_{q',p}}\left\langle n_{q',p} + \frac{1}{2} \mp \frac{1}{2}\right\rangle \delta(\omega \pm \omega_{q',p})\delta(\mathbf{q} \pm \mathbf{q}' - \tau),\end{aligned} \tag{18}$$

where both annihilation and creation of one phonon is considered (represented by the plus and minus sign in the dispersion relation, respectively). In the equation, $\mathbf{e}_{q',p}$ are the polarization unit vectors and $\omega_{q',p}$ the phonon dispersion, b is the nuclear scattering length, M is the atomic mass of the element, $\exp(-2W)$

is the Debye-Waller factor, and $V_0 = \rho_c^{-1}$ is the volume of the unit cell. The sum runs over the polarisation index, p, and the N allowed wave vectors $\mathbf{q}$ within the Brillouin zone (where N is the number of atoms). In addition, the sum runs over the reciprocal lattice vectors, τ, in order to make the dispersion periodic. Further,$\langle n_{q',p}\rangle$ is the Bose factor at the given value of $\hbar|\omega_{q',p}|/(k_B T)$. CHECK OM SUMMEN SKAL LØBE OVER q!

From now, we ignore the q-dependence of the Debye-Waller factor, $\exp(-2W) = const$

GAMMEL TEKST, CHECK OG GENSKRIV DEN NÆSTE HALVE SIDE.

Before calculating $d\sigma/d\Omega$ we need to transform the $\mathbf{q}$ sum into an integral over the Brillouin zone by $\sum_q \to NV_c(2\pi)^{-3}\int_{BZ} d^3\mathbf{q}$. The $\boldsymbol{q}$ sum can now be removed by expanding the $\mathbf{q}$ integral to infinity. All in all, the partial differential cross section reads

$$\begin{aligned}\frac{d^2\sigma'}{d\Omega dE_f}(\boldsymbol{q},\omega) &= b^2\frac{k_f}{k_i}N\frac{1}{2M}\int\frac{\hbar q^2}{c_1|\mathbf{q}-\mathbf{Q}|}\left\langle n_q+\frac{1}{2}\mp\frac{1}{2}\right\rangle\delta(\omega\pm\omega_q)\delta(\boldsymbol{q}\pm\mathbf{q})d^3\mathbf{q}\\ &= b^2\frac{k_f}{k_i}N\frac{\hbar^2q^2}{2Mc_1|\mathbf{q}-\mathbf{Q}|}\left\langle n_q+\frac{1}{2}\pm\frac{1}{2}\right\rangle\delta(\hbar\omega\pm d_1(q)). \qquad (19)\end{aligned}$$

Using the integration sketched in eq. (16), we reach CHECK ISÆR DENNE UDREGNING!

$$\left(\frac{d\sigma'}{d\Omega}\right)_j = b^2\frac{k_f^2}{k_i}N\frac{\hbar^4q^2}{2Mmc_1|\mathbf{q}-\mathbf{Q}|J(k_{f,j})}\left\langle n_q+\frac{1}{2}\pm\frac{1}{2}\right\rangle. \qquad (20)$$

A rough order-of-magnitude consideration gives $\frac{\hbar^2k_{f,j}}{mJ(k_{f,j})}\approx 1$, $\frac{k_{f,j}}{k_{f,i}}\approx 1$, $\langle n_q+\frac{1}{2}\pm\frac{1}{2}\rangle\approx 1$, $\frac{\hbar^2q^2}{2M\hbar\omega_q}\approx\frac{m}{M}$ (for large disperison values?????). Hence, $\left(\frac{d\sigma}{d\Omega}\right)_j\approx Nb^2\frac{m}{M}$, and σ_{inel} becomes a fraction of $4\pi Nb^2$, as one would expect. The differential cross section per unit cell is found from (20) by letting $N=1$. Hence, the weight transformation, Eq. (24), becomes

$$\pi_i = a_{lin}\rho_c l_{max}n_s\Delta\Omega b^2\frac{k_f^2}{k_i}\frac{\hbar^4q}{2Mmc_1|\mathbf{q}-\mathbf{Q}|J(k_{f,j})}\left\langle n_q+\frac{1}{2}\pm\frac{1}{2}\right\rangle, \qquad (21)$$

where the Jacobian reads

$$J = -\frac{\hbar^2}{m}k_f - c\frac{\partial}{\partial k_f}\left|\mathbf{k}_i - k_f\hat{k}_f\right|. \qquad (22)$$

4. The McStas Born-von Karman phonon component

We now proceed to the description of the implementation of phonon scattering in the McStas component `Phonon_BvK`.

4.1. Calculating the weight multiplier

The Mcstas weight multiplier, w, is governed by the rule of sampling probabilities [2]:

$$P = f_{\mathrm{MC}} w, \tag{23}$$

where P is the physical probability of the given event and f_{MC} is the Monte Carlo sampling probability. A "true" physical simulation would always work with having $f_{\mathrm{MC}} = P$ and therefore $w = 1$. A deviation from this will skew the sampling and *e.g.* enlarge the sampling frequency in the cases of interest. In this particular case, we will chose to consider scattering only in a certain solid angle, $\Delta\Omega$.

4.2. Algorithm

TAL OM MCSTAS FOKUSERING

The algorithm for the choice of $\mathbf{k}_{\mathrm{f}}$ reads

1. Check if the ray intersects the sample.
2. Perform a Monte Carlo choice of $\hat{\mathbf{k}}_{\mathrm{f}}$ uniformly, within the solid angle, $\Delta\Omega$.
3. Calculate the possible values of k_{f} that simultaneously fulfills the dispersion relation, $\hbar\omega = d_1(\mathbf{k}_{\mathrm{i}} - k_{\mathrm{f}}\hat{\mathbf{k}}_{\mathrm{f}})$, and the kinematic constraint (BRUG REFERENCE I STEDET?), $\hbar\omega = \hbar^2(k_{\mathrm{i}}^2 - k_{\mathrm{f}}^2)/(2m)$.
4. Choose one of these m values.
5. Calculate $\hbar\omega$ and $\boldsymbol{q}$.
6. Calculate the weight multiplier, π_i, for the scattering event.

As discussed in Ref. [10, p.98], there is always at least one solution for k_{f} to fulfill the dispersion relation, for a given $\hat{\mathbf{k}}_{\mathrm{f}}$, provided the dispersion is continuous and has an upper bound. This is also illustrated in fig. **??**. The weight multiplier is found like in section **??**:

$$\pi_i = a_{\mathrm{lin}} \rho_c l_{\max} m \Delta\Omega \frac{d\sigma}{d\Omega}(\hat{\mathbf{k}}_{\mathrm{f}}). \tag{24}$$

The number of solutions to the dispersion relation, m, has entered this expression. This is because only one solution to the dispersion relation is selected, and the selection is done by a (uniform) Monte Carlo choice. Hence, f_{MC} is reduced by a factor $1/m$, viz. Eq. (**??**).

IMPROVE ON THIS TEXT WHEN CODED

To use the phonon sample, one thus has to supply the parameters $\rho_{\mathrm{c}}, \Delta\Omega, b, V_0, M, T$, and c_1; the attenuation parameters σ_{a} and σ_{inc}; and the parameters describing the size of the sample which is cylinder shaped.

n	$\mathbf{r}_n$	$K_{n,l}$ [N/m]	$K_{n,t}$ [N/m]
1	(a/2 a/2 0)	28.02	-1.57
2	(a 0 0)	0.28	-0.17
3	(a a/2 a/2)	1.11	0.05
4	(a a 0)	0.53	-0.30

Table 1: Born-von Karman force constants for metallic copper, listed as transverse and longitudinal force constants, K_t and K_l, respectively. The lattice constant is $a = 3.597$ Å. Adapted from Ref. [9].

5. Modeling phonons in elemental copper

In 1967, Svensson, Brockhouse, and Rowe published a study of the phonon spectrum in Cu metal [9]. The study was performed at a thermal-neutron triple-axis spectrometer at Chalk River (CAN) and showed very clearly the dispersion relations of the phonon branches in the fcc Bravais lattice of copper; for the main crystal directions separated into transverse and longitudinal vibration modes. In the study, the authors convert their measured dispersion relations into Born-von Karman force constants for up to 8th nearest neighbours. We here deal with the 1'st to 4'th neighbours only and present the force constants in table 1. We see that the dominating force constant is, as expected, the 1'st neighbour longitudinal one.

Figure 1 compares the measured phonon dispersion along the [1 1 0] direction with the results of the Born-von Karman model (4) using the four nearest neighbour interactions. The figure also shows the direction cosines of the three branches, separating the longitudinal branch from the transverse ones along the high-symmetry directions [100], [110], and [111]. We see that the model corresponds to the measurements, with a near-perfect match for most branches, but deviations of the 5% level for the transverse mode along [111]. For a more precise modeling, see the full treatment using forces up to 8'th neighbour in the original publication [9].

DISCUSS MCSTAS DATA.

6. Modeling phonons in pyrolytic graphite

Graphite form a hexagonal lattice structure with four atoms per unit cell (LAV TABEL MED KOORDINATER). The basal (a, b)-planes are identical to graphene, with strong bindings, while the bindings in the c-direction are weak. The most common form of graphite is pyrolytic graphite (PG), where crystalline flakes of graphite are stacked along a common c-direction, but with random stacking disorder in the (a, b)-plane (REFERENCE). Due to its high neutron reflectivity, PG is the most used material for neutron monochromators and analyzers. For a detailed modeling of (thermal diffuse) background scattering from these optical components, it is therefore of large importance to be able to model the phonon spectrum of this material.

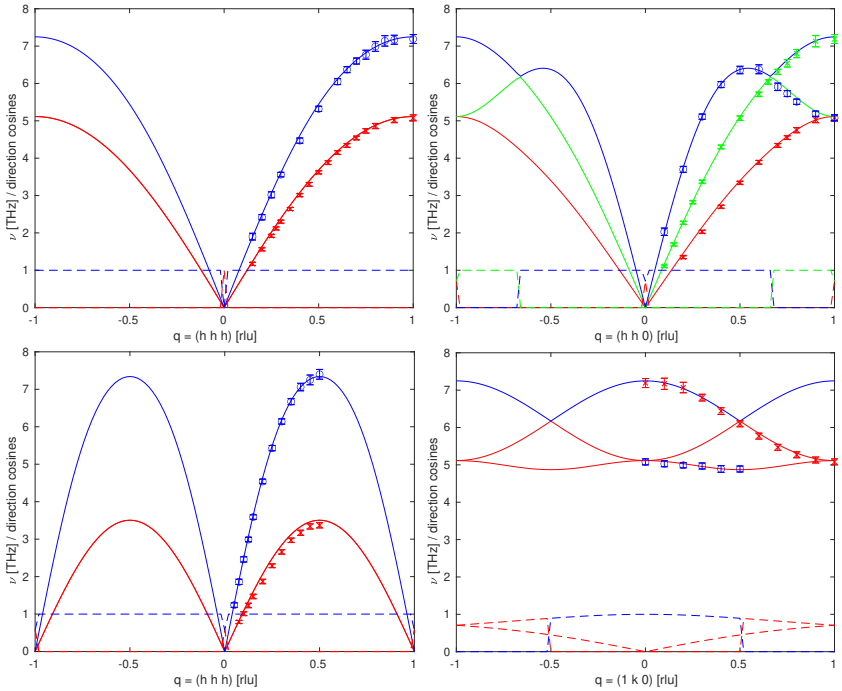

Figure 1: Measured phonon dispersion in Cu (points) along three high-symmetry directions and along [1 k 0]. The full lines show a model of the dispersion calculated from up to 4'th neighbour Born-von Karman force constants, listed in Table 1. The dashed lines show the direction cosines of the three eigenmodes; a value of unity reveals the longitudinal mode.

In 1972, Nicklow, Wakabayashi, and Smith studied the phonon spectrum in PG and modeled it with Born-von Karman theory to 4'th neighbour [11]. Their results are reproduced in Table 2.

Figure 2 compares the measured phonon dispersion along the [0 0 1] and [1 0 0] directions with the results of the Born-von Karman model (4) using only the four nearest neighbour interactions. ?? The figure also shows the direction cosines of the three branches, separating the longitudinal branch from the transverse ones along the high-symmetry directions ??. We see that the model corresponds to the measurements, with a near-perfect match for most branches, but deviations of the 5% level for the transverse mode along [111]. Our modeling results are in perfect agreement with that of the original publication [11].

DISCUSS MCSTAS DATA

7. Conclusion

We have presented an implementation of phonon scattering in McStas, using the Born-von Karman force theory. The resulting McStas component works

n	$\mathbf{r}_n$	$K_{n,l}$ [N/m]	$K_{n,t}$ [N/m]
1	(-a/$\sqrt{3}$ 0 0)	3.62	1.99
2	(0 a 0)	1.33	-0.52
3	(2a/$\sqrt{3}$ 0 0)	-0.037	0.288
4	(0 0 c/2)	0.058	0.0077

Table 2: Born-von Karman force constants for pyrolytic graphite, listed as transverse and longitudinal force constants, K_t and K_l, respectively. The lattice constants are $a = 2.461$ Å and $c = 6.708$ Å. Adapted from Ref. [11].

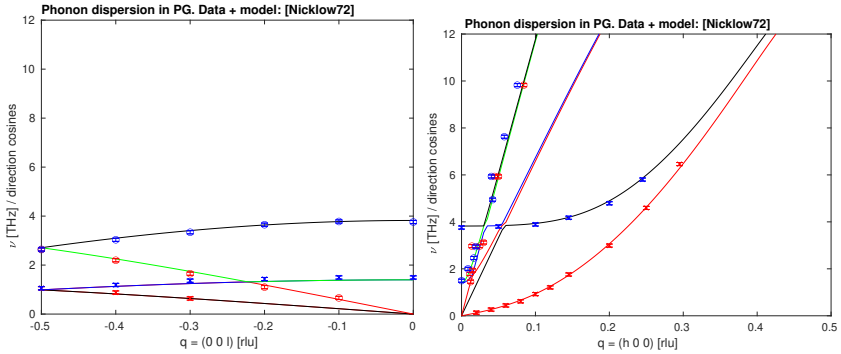

Figure 2: Measured phonon dispersion in Pyrolytic Graphite (points) along the [001] direction (left) and the [100] direction (right). The full lines show a model of the dispersion calculated from up to 4'th neighbour Born-von Karman force constants, listed in Table 2. ?? direction cosines ??

well and efficient and is able to reproduce the literature phonon spectra of two important examples: elemental fcc copper and hexagonal pyrolytic graphite.

(noget mere...)

The scattering algorithm implemented here will be further ported into the McStas `Union` environment and used for the study of thermal diffuse background from analyzer crystals. This work will be the focus of a forthcoming publication [12].

Acknowledgements

We would like to thank Peter Willendrup for decade-long support of the McStas package and the ESS Data Management and Software Center (DMSC) for supplying computing power paramount to the success of this project.

Literature

[1] K. Lefmann, K. Nielsen, McStas, a general software package for neutron ray-tracing simulations, Neutron News 10 (1999) 20–23.

[2] P. K. Willendrup, K. Lefmann, Mcstas (i): Introduction, use, and basic principles for ray-tracing simulations, J. Neutron Res. 22 (2020) 1–16.

[3] P. K. Willendrup, K. Lefmann, Mcstas (ii): An overview of components, their use, and advice for user contributions, J. Neutron Res. 23 (2021) 7–27.

[4] K. Lefmann, P. K. Willendrup, L. Udby, B. Lebech, K. Mortensen, J. O. Birk, K. Klenø, E. Knudsen, P. Christiansen, J. Saroun, J. Kulda, U. Filges, M. Konnecke, P. Tregenna-Piggott, J. Peters, K. Lieutenant, G. Zsigmond, P. Bentley, E. Farhi, Virtual experiments: The ultimate aim of neutron ray-tracing simulations, Journal of Neutron Research 16 (2008) 97–111.

[5] guide_bot GitHub page, https://github.com/mads-bertelsen/guide_bot, 2018.

[6] M. Bertelsen, et al., The union component for mcstas, Nucl. Instr. Meth. A in preparation (2022) –.

[7] E. Farhi, V. Hugouvieux, M. R. Johnson, W. Kob, Virtual experiments: Combining realistic neutron scattering instrument and sample simulations, J. Comp. Phys. 228 (2009).

[8] M. Born, T. von Karman, On fluctuations in spatial grids, Physikalische Zeitschrift 13 (1912) 297–309.

[9] E. C. Svensson, B. N. Brockhouse, J. M. Rowe, Crystal dynamics of copper, Physical Review 155 (1967) 619–632.

[10] G. Squires, Thermal Neutron Scattering, Cambridge University Press, 1978.

[11] R. Nicklow, N. Wakabayashi, H. G. Smith, Lattice dynamics of pyrolitic graphite, Physical Review B 5 (1972) 4951–4962.

[12] K. Krighaar, J. Larsen, R. L. Hansen, J. Lass, J. O. Birk, M. Marko, M. Frontzek, C. Niedermayer, R. T. Petersen, N. B. Christensen, K. Lefmann, Detailed study of the neutron scattering from highly oriented pyrolytic graphite, Rev. Mod. Instr. in preparation (2022) –.